Stimulation-induced changes in $[Ca^{2+}]$ in lizard motor nerve terminals

Gavriel David, John N. Barrett and Ellen F. Barrett

Department of Physiology and Biophysics, R-430, PO Box 016430, Miami, FL 33101, USA

1. Motor axons were injected ionophoretically with one of five Ca^{2+}-sensitive dyes (fluo-3, Calcium Green-2, Calcium Green-5N, fluo-3FF and Oregon Green BAPTA-5N). Changes in fluorescence ($\Delta F/F_{rest}$) within motor terminal boutons following a single action potential and brief stimulus trains were monitored with high temporal resolution using a confocal microscope.

2. Stimulation-induced increases in $\Delta F/F_{rest}$ were confined primarily to boutons, with roughly uniform increases in all the boutons of a terminal. The increase in $\Delta F/F_{rest}$ began prior to, and decayed more slowly than, the endplate potential (EPP) recorded in the underlying muscle fibre. $\Delta F/F_{rest}$ was graded with bath $[Ca^{2+}]$. Both $\Delta F/F_{rest}$ and the EPP were reduced, but not eliminated, by ω-conotoxin GVIA (5–10 μM).

3. For dyes with lower affinity for Ca^{2+} (e.g. Oregon Green BAPTA-5N, $K_d \approx 60$ μM) stimulation-induced increases in $\Delta F/F_{rest}$ were measured in the presence of the K^+ channel blocker 3,4-diaminopyridine (3,4-DAP, 100 μM). During brief stimulus trains (4 at 50 Hz) in 3,4-DAP, the EPP exhibited profound depression, but the fluorescence increase associated with each stimulus showed little decrement, suggesting that depression was not mediated by a reduction in Ca^{2+} entry.

4. For dyes with a higher affinity for Ca^{2+} (e.g. fluo-3, $K_d \approx 0{\cdot}5$–1 μM) stimulation-induced increases in $\Delta F/F_{rest}$ could also be measured in normal physiological saline. Increases in $\Delta F/F_{rest}$ were much greater with 3,4-DAP present, but the amplitude decreased with successive stimuli due to partial dye saturation.

5. Calculations suggested that following a single action potential the average $[Ca^{2+}]$ within a bouton increased by up to 150 nM in normal saline and 940 nM in 3,4-DAP. With low affinity dyes the $\Delta F/F_{rest}$ measured near the membrane had a higher peak amplitude and a faster early decay than that measured in the centre of the bouton, suggesting that substantial spatial $[Ca^{2+}]$ gradients exist within boutons for at least 15 ms following stimulation.

Phasic transmitter release evoked by action potentials requires Ca^{2+} influx into the presynaptic nerve terminal (reviewed by Katz, 1969; Augustine, Charlton & Smith, 1987). Recently it has become possible to measure stimulation-induced changes in intraterminal $[Ca^{2+}]$ ($[Ca^{2+}]_i$) in terminals filled with dyes whose fluorescence properties change upon binding Ca^{2+}. Such studies have revealed that stimulation-induced increases in spatially averaged $[Ca^{2+}]_i$ persist for hundreds of milliseconds or more after stimulation stops, far outlasting phasic evoked release, which is complete within a few milliseconds (Miledi & Parker, 1981; Delaney, Zucker & Tank, 1989; Yawo & Chuhma, 1994; Brain & Bennett, 1995; Borst, Helmchen & Sakmann, 1995; Regehr & Atluri, 1995). At least part of this discrepancy is thought to be due to the existence of spatial $[Ca^{2+}]$ gradients within the stimulated terminal. Modelling studies have estimated spatiotemporal $[Ca^{2+}]_i$ gradients around open Ca^{2+} channels and nearby exocytotic fusion sites, and it has been hypothesized that the rapid time course of phasic evoked transmitter release is due at least in part to transient, localized domains of elevated $[Ca^{2+}]_i$ near release sites (Simon & Llinás, 1985; Yamada & Zucker, 1992; see also Parnas & Parnas, 1994; Klingauf & Neher, 1997). To date the hypothesized spatial gradients and Ca^{2+} domains associated with action potentials have been demonstrated experimentally only at the giant presynaptic terminal of the squid stellate ganglion (Llinás, Sugimori & Silver, 1992). The experiments described here sought to determine whether spatial $[Ca^{2+}]_i$ gradients could also be detected in smaller vertebrate presynaptic terminals.

The rapid line scan of a confocal microscope was used to estimate poststimulation $[Ca^{2+}]_i$ changes occurring in the small (2–5 μm diameter; Melamed & Rahamimoff, 1991) boutons of lizard motor nerve terminals during the first second following stimulation, using intra-axonally injected fluorescent indicator dyes whose estimated K_d values for Ca^{2+} range from ~0·5 to 60 μM. We found marked poststimulation spatial gradients of $[Ca^{2+}]_i$ between the boutons and the preterminal axon. With a high K_d (low affinity) dye it was also possible to demonstrate such gradients within a single bouton. We also estimated the spatially averaged increase in bouton $[Ca^{2+}]_i$ associated with each nerve stimulus. Evidence is presented that the lower affinity dyes produce more accurate estimates of the peak magnitude and early time course of poststimulation $[Ca^{2+}]_i$ changes. We also present simultaneously recorded fluorescence transients and EPPs, which demonstrate that the marked depression of the EPP following stimulation in 3,4-DAP is not due to reduced Ca^{2+} entry. Portions of this work have appeared in abstract form (David, Barrett & Barrett, 1996).

METHODS

Preparation and solutions

Experiments used motor axons innervating the thin ceratomandibularis muscle of small lizards (*Anolis sagrei*). Lizards were captured locally, anaesthetized with ether and killed by decerebration followed by destruction of the brain. The dissected neuromuscular preparation was mounted in a chamber constructed on a thin (no. 1) glass coverslip and placed on the stage of a Nikon inverted microscope. Most experiments used a Nikon ×40 water immersion lens with a numerical aperture of 1·2 and a working distance of 220 μm.

The physiological saline contained (mM): 157 NaCl, 4 KCl, 2 $CaCl_2$, 2 $MgCl_2$, 5 glucose and 1 Hepes; pH 7·3–7·4, adjusted with NaOH. Many experiments used a K^+ channel blocker, 100 μM 3,4-diaminopyridine (3,4-DAP) or (rarely) 5 mM tetraethylammonium (TEA) to prolong the terminal action potential (Brigant & Mallart, 1982; Mallart, 1985; Lindgren & Moore, 1989; Angaut-Petit, Benoit & Mallart, 1989; Morita & Barrett, 1990).

The motor nerve was stimulated by applying brief depolarizing pulses (0·1–0·2 ms, Grass pulse generator) via a suction electrode held by a micromanipulator mounted on the microscope stage. The stimulus intensity was at least three times threshold for eliciting action potentials in normal physiological saline. Carbachol (150–200 μM in physiological saline, up to 600 μM in 3,4-DAP) was added to prevent muscle contraction. We cannot rule out an effect of carbachol on Ca^{2+} entry, but two observations suggest that any such effect is relatively small. First, Morita & Barrett (1989) found that in cut muscle fibre preparations carbachol concentrations in the range 30–100 μM did not alter Ca^{2+}-dependent depolarizations originating in these motor terminals. Second, we found that the early poststimulation fluorescence increase of Ca^{2+} indicator dyes (recorded prior to muscle contraction) was indistinguishable from that recorded in the presence of carbachol. Experiments were performed at room temperature (20–25 °C). ω-Conotoxin GVIA was purchased from Calbiochem or Research Biochemicals International. All other reagents were from Sigma.

Dye injection into axons

Microelectrodes for dye ionophoresis were pulled with a Brown-Flaming puller (Sutter Instrument Co., Novato, CA, USA). Tips were backfilled with potassium salts of one of the following dyes: fluo-3, Calcium Green-2, Calcium Green-5N, Oregon Green BAPTA-5N, and fluo-3FF, diluted in water to a concentration of 1–4 mM. The first four dyes were from Molecular Probes; fluo-3FF was from Texas Fluorescence Labs (Teflabs), Austin, TX, USA. Electrode barrels were filled with 3 M KCl. The resistances of filled electrodes ranged from 100 to 300 MΩ.

Axons were impaled using a piezoelectric device to 'tap' the microelectrode through the myelin sheath into the axon. Successful impalements yielded a resting potential at least as hyperpolarized as −60 mV and an action potential following stimulation of the motor nerve. Dyes were injected ionophoretically by applying continuous negative currents (0·5–1·5 nA) through the intra-axonal dye-filled electrode. Successful injections achieved dye concentrations sufficient for fluorescence measurements after 15–35 min of ionophoresis, after which the electrode was withdrawn from the axon. Normalized poststimulation fluorescence transients recorded from intensely fluorescent terminals near the injection site were not detectably different from those recorded from weakly fluorescent terminals of the same axon farther from the injection site, suggesting that the indicator dye concentrations used here did not produce a major distortion of the $[Ca^{2+}]_i$ transient. Also, the stimulation-induced $[Ca^{2+}]_i$ elevation in dye-injected terminals remained sufficient to produce suprathreshold EPPs in the underlying muscle fibres.

Fluorescence measurements

Dye properties. Fluo-3 and Calcium Green-2 have relatively high affinities for Ca^{2+}, with reported K_d values ranging from 0·4 to 2 μM. Oregon Green BAPTA-5N and fluo-3FF have relatively low affinities for Ca^{2+}, with K_d values of ~60 and ~42 μM, respectively (mean of 4 determinations for each dye at room temperature, pH 7·0, mammalian (= reptilian) ionic strength; W. G. L. Kerrick, personal communication). Reported K_d values for Calcium Green-5N range from 3·3 to 67 μM; this dye may have more than one type of Ca^{2+}-binding site (Ukhanov, Flores, Hsiao, Mohapatra, Pitts & Payne, 1995; W. G. L. Kerrick, personal communication).

Dyes were excited with the 488 nm line of an argon laser (Omnichrome, Chino, CA, USA). Emissions were monitored with a 515 nm long-pass filter (Omega Optical, Brattleboro, VT, USA).

Image collection and analysis. Images were collected with an Odyssey XL confocal microscope (Noran Instruments, Middleton, WI, USA). Measurements requiring the fastest time resolution used the line scan mode, in which each point on a line is sampled once every 69 μs (pixel dwell time, 100 ns; line scan of 620 pixels repeated 479 times in 33 ms; see Fig. 2*C*). We usually collected three to ten sequential line scan images spanning intervals before and after a short train of stimuli. At the end of each image (spanning 33 ms) there was a computer-generated delay equivalent to about forty-eight lines (3·3 ms), indicated as a break in the plotted records (e.g. Figure 2*D*).

Measurements of average pixel intensity within a given area used the whole image mode (image of 620 × 479 pixels completed in 33 ms). Up to eighty sequential images were collected before, during and after stimulus trains (as in Fig. 1).

To correlate electrophysiological and imaging records, nerve stimulation was triggered by a pulse from the confocal microscope,

with a delay that allowed acquisition of 200–350 control sweeps (line scan mode) or five to twenty control images (whole image mode) before the nerve was stimulated. In the line scan mode the pulse that stimulated the nerve also triggered a light-emitting diode mounted just above the microscope condenser, yielding an optical signal to mark the time of stimulation (visible in e.g. Fig. 2*C*). The light pulse emitted by the diode had sharp on–off edges (completed within 1 line scan).

Pixel intensity data were collected using an Indy workstation (Silicon Graphics) with Noran InterVision software. Data files were converted to TIFF format using a custom Pascal program (written by G.D.), and transferred via a local network to a Pentium computer. Image data were stored on removable 1·2 Gb erasable optical disks using a Sierra disk drive (Pinnacle Micro, Irvine, CA, USA). Imaging data are plotted as $\Delta F/F_{rest}$ (usually abbreviated as $\Delta F/F$), where ΔF is the change in fluorescence and F_{rest} is resting (pre-stimulation) fluorescence. F_{rest} was corrected for the mean background fluorescence, which was calculated off-line. Data plots were prepared using Coplot (CoHort Software, Berkeley, CA, USA).

Estimation of stimulation-induced changes in average bouton $[Ca^{2+}]_i$

It was difficult to estimate changes in $[Ca^{2+}]_i$ from fluorescence increases in motor terminals using calibration techniques developed for isolated cells in culture, for reasons detailed in David, Barrett & Barrett (1997). Stimulation-induced changes in average bouton $[Ca^{2+}]_i$ were instead estimated from measured $\Delta F/F_{rest}$ values using approaches based on the following equation from Grynkiewicz, Poenie & Tsien (1985):

$$[Ca^{2+}]_i = K_d(F_{meas} - F_{min})/(F_{max} - F_{meas}), \quad (1)$$

where K_d is the dissociation constant for the calcium–dye complex, F_{meas} is the measured (background-subtracted) fluorescence, and F_{min} and F_{max} are the minimal and maximal dye fluorescence. Modifications of eqn (1) used for high and low affinity dyes are described in the legend to Table 1.

Correction for kinetics of Ca^{2+} binding to dyes

Equation (1) assumes kinetic equilibrium between free Ca^{2+}, free dye, and the Ca^{2+}–dye complex (which determines the measured fluorescence). But because these dyes bind Ca^{2+} with finite kinetics, this assumption is not true at the earliest poststimulus times. This temporary disequilibrium results in an underestimate of the peak $\Delta[Ca^{2+}]_i$, and also slows the early decay of the calculated $[Ca^{2+}]_i$ transient. A correction for the contribution of dye kinetics can be obtained by adding a derivative term to eqn (1) as follows:

$$[Ca^{2+}]_i = K_d\frac{(F_{meas} - F_{min})}{(F_{max} - F_{meas})} + \frac{K_d\tau_{off}\frac{dF_{meas}}{dt}}{(F_{max} - F_{meas})}, \quad (2)$$

where τ_{off} is the time constant for dissociation of Ca^{2+} from the dye. Calculations used τ_{off} of 2·4 ms for fluo-3 (Lattanzio & Bartschat, 1991), and 0·04 ms for Oregon Green BAPTA-5N, assuming that the ~60-fold difference in the K_d values of these dyes is attributable mainly to differences in τ_{off} (the association between Ca^{2+} and these dyes, both of which are BAPTA derivatives, is so rapid as to be essentially diffusion limited). Equation (2) assumes a spatially uniform compartment; spatial gradients of $[Ca^{2+}]_i$ within the bouton will lead to an underestimate of $[Ca^{2+}]_i$ in regions of greatest $[Ca^{2+}]_i$ increase. This equation was applied to the fluo-3 and Oregon Green BAPTA-5N $\Delta F/F$ transients of Fig. 7*A* and *B*, using assumptions described in the legend to Table 1. Because the derivative term in eqn (2) is very sensitive to noise fluctuations, calculations were performed on smoothed curves fitted by eye to the $\Delta F/F$ transients.

Electrophysiological measurements

EPPs were recorded with a microelectrode inserted into the muscle fibre underlying the imaged terminal. These microelectrodes were pulled from borosilicate glass with a Brown-Flaming puller and filled with 3 M KCl (resistance 5–10 MΩ). Electrical signals were fed into an Axoclamp-2B preamplifier (Axon Instruments) and thence into a custom ×10 amplifier with built-in offset adjustment. Signals from the amplifier were monitored on a digital oscilloscope (model 54603B, Hewlett Packard) and fed into a 16 bit analog-to-digital converter (Analogic, Wakefield, MA, USA) sampling at 10 kHz for storage on a 486 computer. EPPs were averaged using Snap-Master 3.1 software (HEM Data Corp., Southfield, MI, USA).

RESULTS

Distribution of Ca^{2+} within stimulated terminals

Figure 1 shows $\Delta F/F$ transients from a Calcium Green-5N-filled motor terminal and preterminal axon stimulated at 50 Hz for 1 s in the presence of 3,4-DAP. The upper fluorescence micrograph in Fig. 1*A* shows the terminal (whole-image mode); the lower micrograph shows this terminal with red arrows marking analysed boutons, and numbered green arrows marking regions of preterminal axon. The $\Delta F/F$ transients of these marked regions are plotted in Fig. 1*C*. Figure 1*B* shows pseudocolour images of the terminal before stimulation and at various times during and after stimulation. These pictures and the $\Delta F/F$ transients plotted in red show that the stimulation-induced fluorescence increase (and thus the increase in $[Ca^{2+}]_i$) was similar in all terminal boutons. This uniformity in the $\Delta F/F$ transients recorded in the boutons of a given terminal was also observed using different dyes, in the presence or absence of K^+ channel blockers, and with the faster line scan sampling mode (where the scanned line passed through multiple boutons).

$\Delta F/F$ transients recorded in the transition region between the terminal and the pre-terminal heminode (numbered green traces in Fig. 1*C*) rose more slowly, and a substantial gradient between the preterminal axon and terminal boutons persisted throughout the stimulus train. Even during this prolonged stimulation there was little increase in the fluorescence of the last myelinated segment of the axon (trace 4). Restriction of the $\Delta F/F$ increase to boutons was not an artifact of dye injection, because similar results were obtained with all dyes tested (K_d values ranging from ~1 to 60 μM), and over a wide range of intracellular dye concentrations (as inferred from resting fluorescence intensities). In fact, because the calcium–dye complex may diffuse faster than free Ca^{2+}, the records in Fig. 1 may even underestimate the degree to which the stimulation-induced increase in $[Ca^{2+}]_i$ is confined to terminal boutons.

Another experiment (not shown) examined the spread of Ca^{2+} in the reverse direction, from the preterminal region

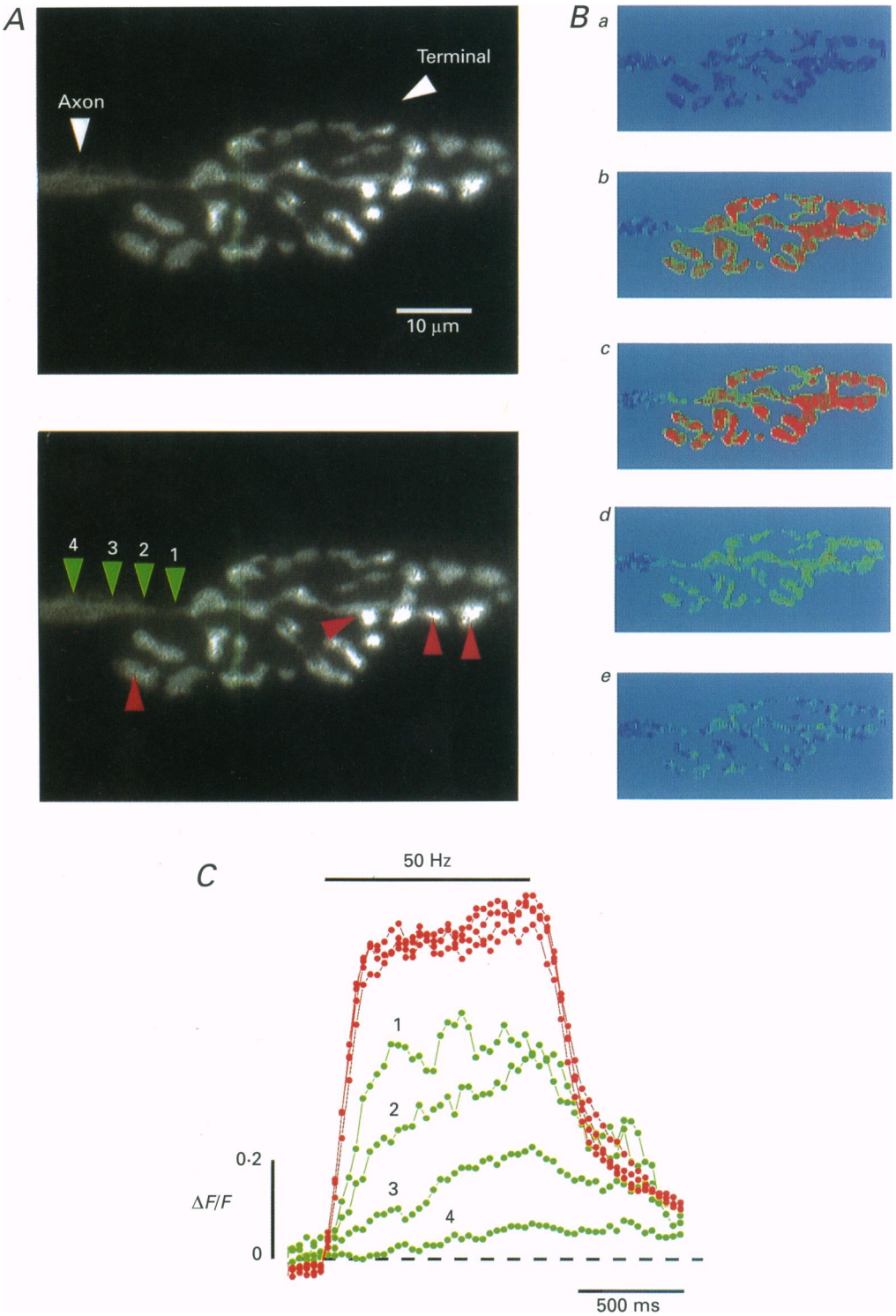

Figure 1. Stimulation-evoked increases in fluorescence in a terminal filled with Calcium Green-5N and stimulated for 1 s at 50 Hz in 100 μM 3,4-DAP and 600 μM carbachol

A, fluorescence images of the terminal (upper image, whole-image mode, average of 20 images). Bouton and axonal regions analysed in *C* are marked in the lower image. *B*, pseudocolour images (red indicates largest increase in $\Delta F/F$) taken before (*a*), 165 ms (*b*) and 825 ms (*c*) after stimulation began, and 155 ms (*d*) and 617 ms (*e*) after stimulation ended. *C*, time course of changes in $\Delta F/F$ in 4 boutons (red) and in several regions of the preterminal axon (numbered green traces). The time series was obtained by analysing 60 images collected over a 2 s interval that included the stimulus train (indicated by upper horizontal bar). The average pixel intensity within each region was calculated using InterVision software. In this and subsequent figures most $\Delta F/F$ transients were smoothed using a moving bin technique (5–10 points per average).

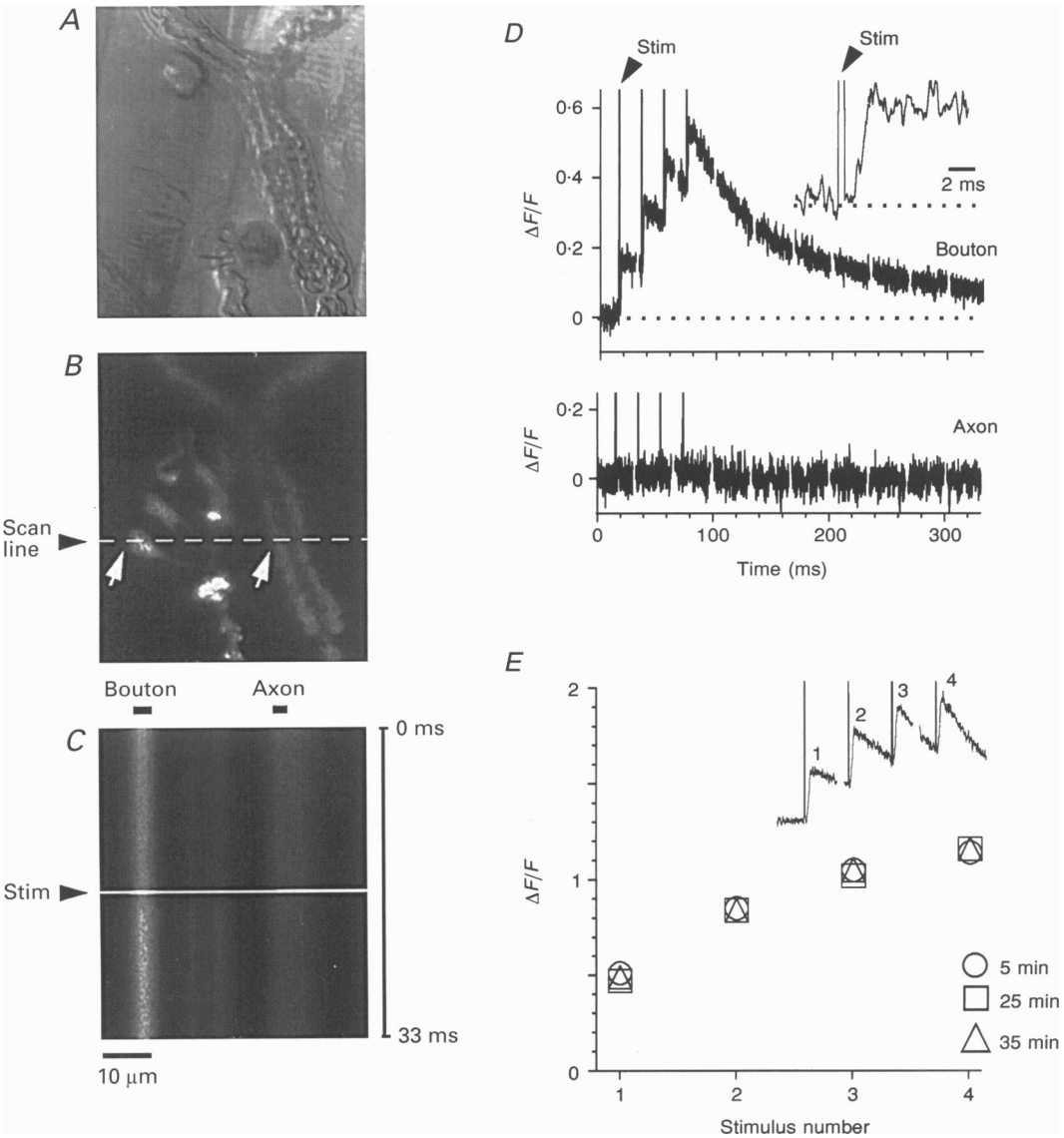

Figure 2. Stimulation-evoked fluorescence changes in motor axon and terminal bouton filled with Oregon Green BAPTA-5N

A and *B*, phase and fluorescence micrographs of dye-injected axon. The myelinated axon bifurcated at the node shown at lower right, and one of the daughter branches gave rise to the imaged motor terminal. Dashed line in *B* indicates the location of the scan, with arrows indicating the bouton (left) and axon (right) indicated in *C*. *C*, sequential measurements of fluorescence along the line indicated in *B* (time increases from top to bottom, indicated by scale at right) before and after the first stimulus in a 4-impulse 50 Hz train. This image is an average of 50 repetitions, each consisting of a total of 479 scans collected over a 33 ms interval. The white horizontal line was produced by a light-emitting diode triggered at the time of nerve stimulation. Bars at top indicate the width of bouton and axon over which intensity was averaged (using custom macros written with PMIS software (Photometrics, Tucson, AZ, USA)) to produce the records plotted in *D*. Calibration bar in *C* applies also to *A* and *B*. *D*, time course of fluorescence changes ($\Delta F/F$, background-subtracted) in the bouton (upper) and axon (lower) indicated in *C*, averaged from 50 repetitions of a 4-impulse, 50 Hz train delivered at 30 s intervals. Plotted records show 10 sequential line scan images (data in *C* contributed to the average during the first 33 ms); discontinuities in the record mark the transition between successive images. Inset in *D* shows the onset of the response to the first stimulus on an expanded time scale. *E*, peak $\Delta F/F$ as a function of stimulus number for another motor terminal filled with Oregon Green BAPTA-5N and stimulated in the same pattern as in *D*. Symbols plot the peak $\Delta F/F$ averaged from sets of 10 trains collected 5, 25 and 35 min following the onset of stimulation, showing that the $\Delta F/F$ values were stable over time. The inset plots the time course of $\Delta F/F$ transients averaged from 70 stimulus trains. All records were collected in the presence of 100 μM 3,4-DAP and 600 μM carbachol.

into the boutons of a fura-2-filled axon, using ratiometric imaging techniques as in David *et al.* (1997). Large negative current pulses were applied through an electrode in the myelin sheath about 150 μm from the terminal to produce a localized dielectric breakdown of the axonal membrane. The resulting increase in $[Ca^{2+}]_i$ spread slowly over several minutes from the axon into some terminal boutons, with substantial $[Ca^{2+}]_i$ gradients maintained between the axon and some boutons. These gradients are likely to be due to the diffusion barrier posed by the small diameter ($\leqslant 1$ μm) of the process connecting the terminal regions to the myelinated axon, as well as to the Ca^{2+} buffering/sequestration/extrusion capacity of motor terminals.

Stimulation-induced fluorescence changes with low affinity dyes

Figure 2 shows typical results obtained using the faster line scan mode with a low affinity dye, Oregon Green BAPTA-5N, in the presence of 3,4-DAP. Figure 2*A* and *B* show, respectively, phase and fluorescence micrographs of portions of a dye-filled axon and motor nerve terminal; the dashed line in Fig. 2*B* passes through myelinated portions of the axon and a synaptic bouton. Figure 2*C* is an averaged line scan image showing (from top to bottom) fluorescence measurements obtained by scanning this line repeatedly (every 69 μs) before and after the first of four stimuli

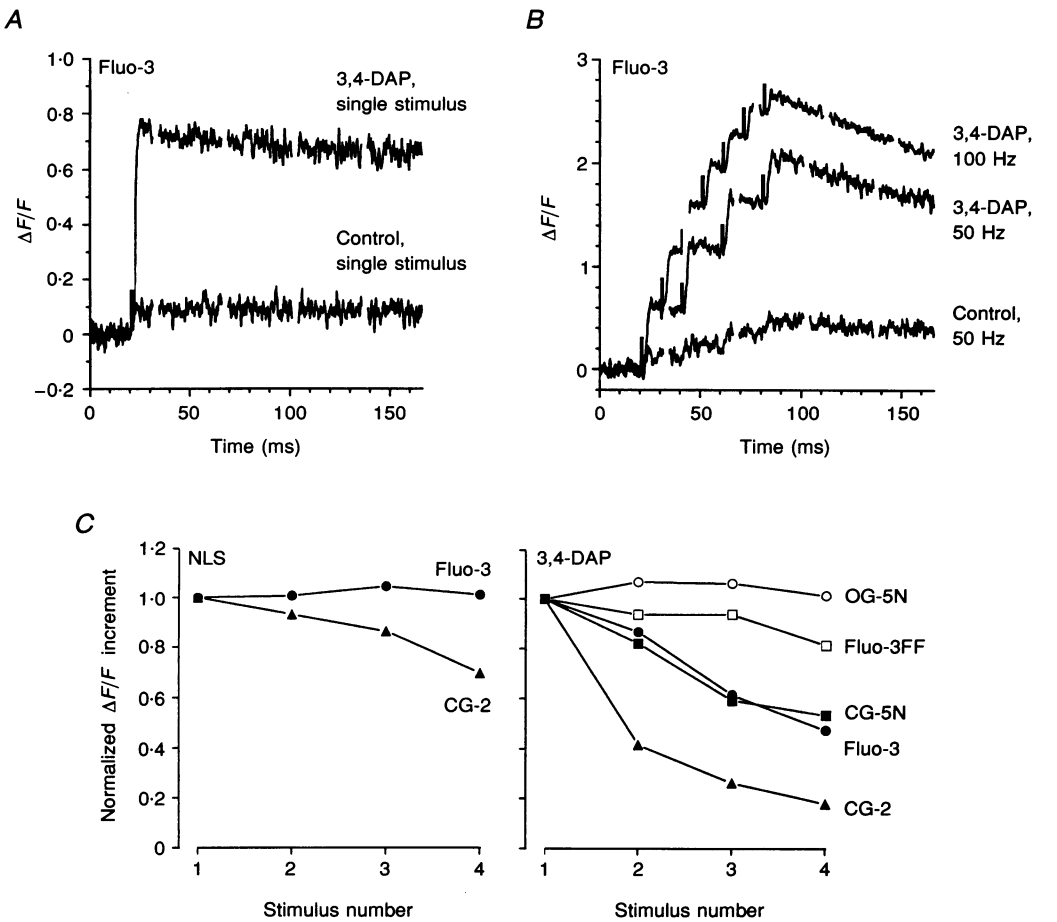

Figure 3. Stimulation-evoked changes in bouton fluorescence measured using high or low affinity dyes in the presence or absence of 3,4-DAP

A, average response to single stimuli in a fluo-3-filled bouton before (control, $n = 50$ trials) and 30 min after addition of 100 μM 3,4-DAP ($n = 72$). *B*, response to 4 stimuli at 50 Hz or 7 stimuli at 100 Hz before and after addition of 3,4-DAP in the same terminal as *A* ($n = 20$–50; trains repeated every 30 s). [Carbachol], 300 μM in *A* and *B*. *C*, average peak increment in fluorescence produced by the first 4 stimuli in a 50 Hz train, normalized to the increase produced by the first stimulus (see below), for the indicated dyes in the absence (left) or presence (right) of 100 μM 3,4-DAP (NLS indicates normal lizard saline; CG and OG indicate Calcium and Oregon Green, respectively). The peak increment was calculated as the difference between the peak $\Delta F/F$ recorded after, and the $\Delta F/F$ value recorded just before, the indicated stimulus. Mean peak increments in response to the first stimulus in NLS were 0·1 for CG-2 and 0·3 for fluo-3; and in 3,4-DAP, 0·8 for CG-2, 1·6 for fluo-3, 0·27 for CG-5N, 0·12 for fluo-3FF and 0·33 for OG BAPTA-5N ($n = 2$–30 boutons in at least 2 different preparations for each condition). All solutions contained carbachol at a concentration sufficient to block muscle contraction (200–600 μM).

Table 1. Spatially averaged increases in $[Ca^{2+}]_i$ associated with a single nerve stimulus, calculated from $\Delta F/F$ measurements

Dye	[3,4-DAP] (μM)	$\Delta[Ca^{2+}]_i$ (nM)
Fluo-3*	0	20–80
Calcium Green-2†	0	4–16
Oregon Green BAPTA-5N‡§	0	30–150
Fluo-3*	100	90–450
Fluo-3†	100	20–90
Calcium Green-2†	100	50–200
Oregon Green BAPTA-5N‡	100	170–940

In all calculations the assumed range of resting $[Ca^{2+}]_i$ was 50–100 nM. * For fluo-3 eqn (1) in Methods was modified to:

$$[Ca^{2+}]_i = K_d[(\Delta F/F_{rest}) + 1]/[(K_d/[Ca^{2+}]_{rest}) - (\Delta F/F_{rest})],$$

assuming $F_{min} = 0$ (Cheng, Lederer & Cannell, 1993) and $K_d = 0{\cdot}3$–$1{\cdot}5$ μM. †For dyes that show a decrementing ΔF for successive stimuli during a train:

$$\Delta[Ca^{2+}]_i = ([Ca^{2+}]_{rest} + K_d)(1 - \alpha)/2\alpha,$$

where α = (peak increase in ΔF associated with second stimulus)/(peak increase in ΔF associated with first stimulus; Feller, Delaney & Tank, 1996). K_d estimates as above. The assumption that the decrement in the recorded signal is due solely to partial dye saturation is supported by the lack of a decrement for the low affinity dye Oregon Green BAPTA-5N (Figs 2*D* and 3*C*). The assumption that the decay of fluorescence during the first interstimulus interval is negligible is supported by Fig. 3*B*. ‡For Oregon Green BAPTA-5N:

$$\beta = F_{rest}/F_{min} = (K_d + ([Ca^{2+}]_{rest})(F_{max}/F_{min}))/(K_d + [Ca^{2+}]_{rest}),$$

and the value of β should be only slightly greater than 1. Equation (1) then becomes:

$$[Ca^{2+}]_i = K_d[(\Delta F/F_{rest} + 1 - 1/\beta)/(F_{max}/F_{rest} - \Delta F/F_{rest} - 1)].$$

K_d range, 30–70 μM; F_{max}/F_{min} range, 30–70 (ratio of 50 measured by W. G. L. Kerrick, personal communication). §Based on $\Delta F/F_{rest} = 0{\cdot}04$ measured in one Oregon Green BAPTA-5N-filled terminal in NLS.

delivered at 50 Hz to the motor nerve. The fluorescence of the bouton increased shortly after stimulation. Figure 2*D* plots the average time course of $\Delta F/F$ transients recorded during and after the four-stimulus train in this bouton (upper) and axon (lower), obtained from ten sequential sets of line scan images. The inset shows the early time course in the bouton. Each stimulus in the train produced a roughly equal step increase in bouton fluorescence. No stimulation-induced fluorescence increases were detected in the axon. This record also indicates that the line scan produced no detectable dye bleaching.

The inset in Fig. 2*E* shows $\Delta F/F$ transients averaged from seventy trials in a bouton of another motor terminal injected with Oregon Green BAPTA-5N and similarly stimulated. Plotted symbols show the peak $\Delta F/F$ after each stimulus in the train, averaged for groups of ten trials obtained 5, 25 and 35 min following the onset of stimulation. The close overlap of the points indicates good stability, and suggests that the increase in $[Ca^{2+}]_i$ elicited by the four-impulse train had decayed completely before the onset of the next train.

For both low affinity dyes (Oregon Green BAPTA-5N and fluo3-FF) the magnitude of the step increase in $\Delta F/F$ did not change for subsequent stimuli in the train. Most experiments with low affinity dyes were performed in 3,4-DAP because in the absence of a K^+ channel blocker the increase in fluorescence following a single stimulus was difficult to measure accurately (peak $\Delta F/F \leqslant 0{\cdot}05$).

Stimulation-induced fluorescence changes with high affinity dyes

Fluorescence increases in the absence of K^+ channel blockers could be detected using dyes with a higher affinity for Ca^{2+}, fluo-3 and Calcium Green-2. Figure 3*A* and *B* compares $\Delta F/F$ transients recorded in response to single and short trains of stimuli with fluo-3 in the presence and absence of 3,4-DAP. Responses in the presence of 3,4-DAP or 5 mM TEA (not shown) were consistently greater than those recorded in their absence.

With the high affinity dyes the peak stimulation-induced increase in $\Delta F/F$ decreased with successive stimuli in the presence of K^+ channel blockers. This decrementing

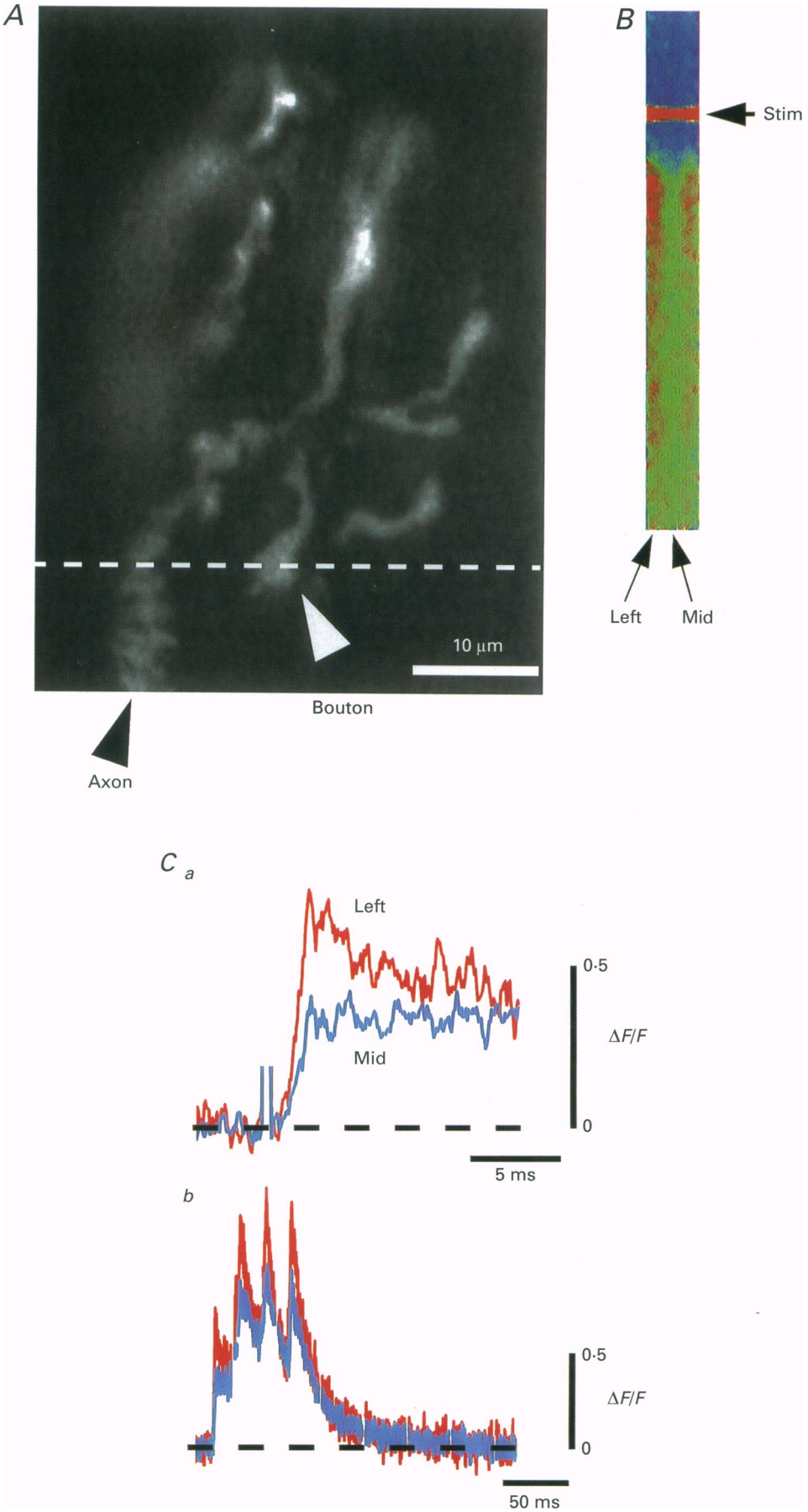

Figure 4. Differences in $\Delta F/F$ transients measured at the edges and centre of a single bouton

A, fluorescence micrograph showing motor terminal filled with Oregon Green BAPTA-5N (average of 32 images collected in whole image mode). *B*, segment of line scan image corresponding to the first stimulus delivered to the bouton indicated in *A*. Scans were converted (after spatial binning) to a pseudocolour $\Delta F/F$ image (red marks stimulus (horizontal line) and greatest poststimulus $\Delta F/F$). This line scan image covers the same time interval as the plot in *Ca*. *Ca*, time course of changes in $\Delta F/F$ after the first stimulus in a train for the left (red) and middle (blue) thirds of the bouton shown in *A* and *B* (average of 40 repetitions). *Cb*, similar plot constructed with a slower time axis to include the full 4-stimulus train and the post-train decay. Trains were repeated at 30 s intervals. [3,4-DAP], 100 μM ; [carbachol], 600 μM .

behaviour was apparent in all boutons sampled in the presence of K^+ channel blockers in Calcium Green-2 ($n = 6$ boutons in 3,4-DAP, $n = 5$ in TEA) and in fluo-3 ($n = 3$ in 3,4-DAP), as summarized in the averaged data plotted in Fig. 3*C* (right). Decrements with successive stimuli were much less pronounced in the absence of K^+ channel blockers (Fig. 3*C* left).

The findings that little or no decrement in the $\Delta F/F$ increase was seen with low affinity dyes and that the decrement observed with high affinity dyes was less in the absence than in the presence of K^+ channel blockers suggest that the decrement seen with high affinity dyes was due to dye saturation rather than to a progressive decrease in Ca^{2+} entry with successive stimuli. Similar conclusions were reached by Regehr & Atluri (1995) in their study of stimulation-induced fluorescence transients using high and low affinity dyes in cerebellar granule cell presynaptic terminals.

Another dye, Calcium Green-5N, yielded $\Delta F/F$ transients with properties intermediate between those measured for the high and low affinity dyes. Like the low affinity dyes, Calcium Green-5N yielded little or no detectable fluorescence increase in response to brief stimulus trains in the absence of K^+ channel blockers. As for the high affinity dyes, the peak increase in $\Delta F/F$ for Calcium Green-5N decreased with successive stimuli (see averaged response in Fig. 3*C*, $n = 23$). The intermediate behaviour observed with Calcium Green-5N is attributable to its intermediate K_d and possibly to multiple Ca^{2+} binding sites (see Methods).

Estimation of stimulation-induced elevation of $[Ca^{2+}]_i$ in lizard motor boutons

Table 1 shows estimates of the spatially averaged increment in bouton $[Ca^{2+}]_i$ calculated from averaged data like those in Figs 2 and 3. These calculations suggest that a single stimulus increases average bouton $[Ca^{2+}]_i$ by up to 150 nM in the absence of K^+ channel blockers, and by up to 940 nM in the presence of 3,4-DAP. The increments in bouton $[Ca^{2+}]_i$ estimated using the low affinity dye Oregon Green BAPTA-5N were greater than those estimated using the higher affinity dyes fluo-3 and Calcium Green-2 (see Discussion).

Poststimulation spatial gradient within boutons

The values in Table 1 underestimate the peak stimulation-induced increase in bouton $[Ca^{2+}]_i$ at early times and near sites of Ca^{2+} influx (see Discussion). One reason for this underestimate is illustrated in Fig. 4, which demonstrates a spatial $\Delta F/F$ gradient at early poststimulation times in a bouton (diameter, ~4 μm; Fig. 4*A*) filled with Oregon Green BAPTA-5N. The line scan image, converted to a pseudocolour $\Delta F/F$ image (Fig. 4*B*), indicates that at early times the increase in $\Delta F/F$ was greater near the edges of the

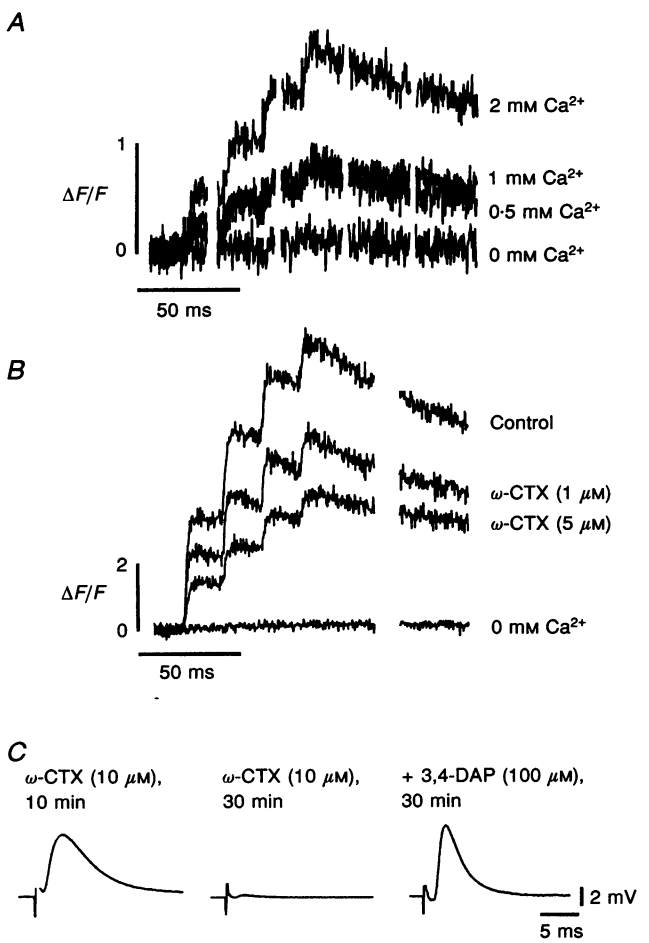

Figure 5. Effects of bath $[Ca^{2+}]$ (*A*) and ω-conotoxin GVIA (*B* and *C*)

A and *B* show $\Delta F/F$ transients from line scans of fluo-3-filled boutons stimulated at 50 Hz. Traces in *A* show averages of 10 trials recorded in the indicated bath $[Ca^{2+}]$. Traces in *B* are averages of 20 trials recorded (top to bottom) in normal lizard saline (control), 65 min after addition of 1 μM ω-conotoxin GVIA, 54 min after increasing toxin concentration to 5 μM, and 37 min after washing the preparation with a solution containing no added Ca^{2+} and 6 mM Mg^{2+}. Traces in *B* used a slower line scan than in *A* and no spatial binning. *C*, EPPs averaged from a different endplate 10 min (left) and 30 min (middle) after addition of 10 μM ω-conotoxin GVIA, and 30 min after adding 3,4-DAP to the toxin-containing solution (right, $n = 10$ for each condition). Similar changes in EPP amplitude were recorded in the endplate under the terminal in *B*. [Carbachol], 150 μM in *A*, 600 μM in *B*, none in *C*; [3,4-DAP], none in *A* and left and middle traces in *C*, 100 μM in *B* and right trace in *C*.

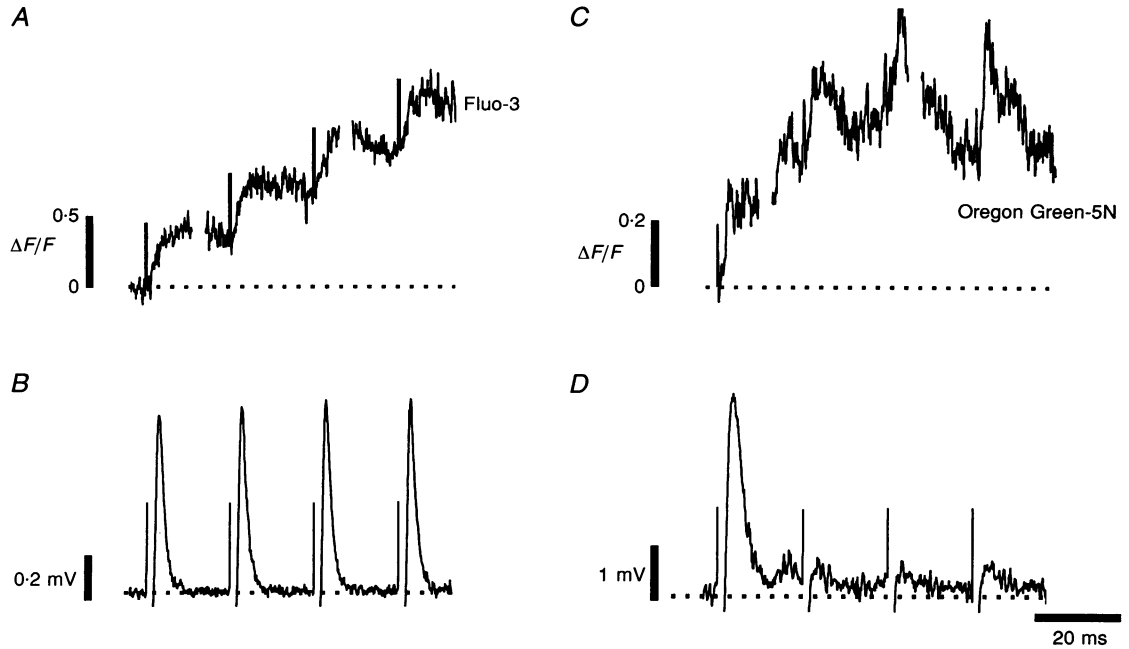

Figure 6. $\Delta F/F$ transients and EPPs recorded simultaneously during repetitive stimulation in the absence (*A* and *B*) or presence (*C* and *D*) of 100 μM 3,4-DAP

In the normal saline record, obtained with a fluo-3 loaded terminal, neither the $\Delta F/F$ transient (*A*) nor the EPP (*B*) decreased significantly during repetitive stimulation. In the record obtained in 3,4-DAP with an Oregon green BAPTA 5N-loaded terminal, the EPP decreased markedly during repetitive stimulation (*D*), but the $\Delta F/F$ transient did not (*C*). The EPP in response to the first stimulus was larger in *D* than in *B* (even though more carbachol was present in *D*), suggesting increased transmitter release in 3,4-DAP. *C* and *D* show evidence of an additional spontaneous discharge between the first and second stimuli, a phenomenon sometimes observed with aminopyridines. Traces are averages of 30 (*A*), 10 (*B*), and 5 trials (*C* and *D*). [Carbachol], 100 μM in *A* and *B*, 300 μM in *C* and *D*.

bouton (especially the left edge) than in the middle of the bouton. This gradient is in the direction expected for influx of Ca^{2+} through membrane channels. Figure 4*C* plots the time course of poststimulation changes in $\Delta F/F$ averaged over the left and middle thirds of this bouton. After the first stimulus (upper plot) a difference between edge and middle values was detectable for at least the first 15 ms following stimulation. This gradient is unlikely to be simply an artifact due to edge effects or improper normalization, because light was averaged over equivalent distances for both the edge and centre $\Delta F/F$ calculations, and because the edge and centre $\Delta F/F$ values converged at later times. The lower plot in Fig. 4*C* shows on a slower time scale that qualitatively similar edge-to-middle $\Delta F/F$ differences could

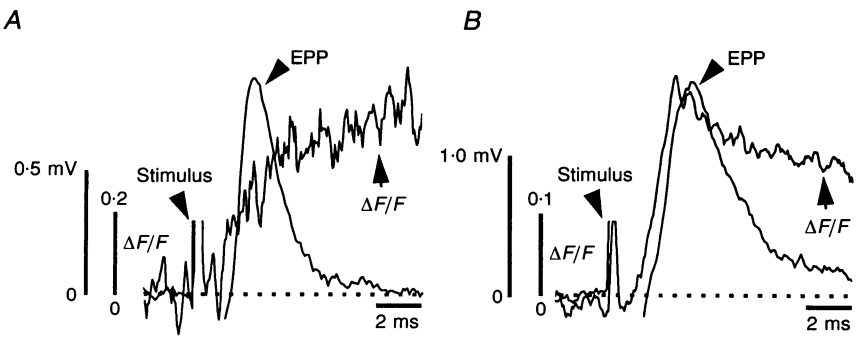

Figure 7. Early time course of simultaneously recorded average EPP and fluorescence transients in terminals loaded with fluo-3 (*A*) or Oregon Green BAPTA-5N (*B*)

Records were aligned at the onset of the stimulus artifact. Traces are the averages of 17 (EPP and $\Delta F/F$ in *A*), 42 (EPP in *B*) and 50 trials ($\Delta F/F$ in *B*). $\Delta F/F$ in *A* is the average of 2 boutons in the same terminal. [Carbachol], 150 μM in *A*, 300 μM in *B*; [3,4-DAP], 100 μM in *B*. Muscle resting potential, − 60 mV in *A*, −69 mV in *B*.

be detected for each stimulus in the train, with the values converging at later times following the train. Poststimulus spatial $\Delta F/F$ gradients were also detected in terminals filled with Calcium Green-5N, but were more difficult to detect in boutons filled with the higher affinity dye fluo-3 (see Discussion).

Fluorescence changes are graded with bath $[Ca^{2+}]$ and reduced by ω-conotoxin

Figure 5*A* shows $\Delta F/F$ transients measured in a bouton filled with fluo-3, demonstrating that the magnitude of the recorded transients decreased as bath $[Ca^{2+}]$ was reduced. The fact that the transient recorded in 0·5 mM Ca^{2+} was not detectably smaller than that recorded in 1 mM Ca^{2+} may be attributable simply to a decreasing signal-to-noise ratio. Another possible explanation is that the duration of the terminal action potential increased as bath $[Ca^{2+}]$ decreased, since lizard motor terminals have a charybdotoxin-sensitive, Ca^{2+}-dependent K^+ conductance that contributes to action potential repolarization (Angaut-Petit *et al.* 1989; Lindgren & Moore, 1989; Morita & Barrett, 1990).

Figure 5*B* plots $\Delta F/F$ transients recorded in a fluo-3-loaded bouton in 3,4-DAP before (control) and following addition of 1 and 5 μM ω-conotoxin GVIA, a blocker of N-type Ca^{2+} channels. The toxin produced a concentration-dependent reduction in the $\Delta F/F$ transient, but a substantial signal persisted even after prolonged toxin exposure. This toxin-resistant component was Ca^{2+} dependent, as evidenced by its disappearance when Ca^{2+} was removed from the bath. Preliminary experiments indicated that the toxin-resistant component was not reduced by 1 μM nimodipine, which blocks L-type Ca^{2+} channels. In another preparation filled with the lower affinity dye Calcium Green-5N, 1 μM ω-conotoxin GVIA almost completely eliminated the recorded $\Delta F/F$ transient (not shown).

Figure 5*C* shows averaged EPPs recorded from a different endplate exposed to 10 μM ω-conotoxin GVIA in the absence of carbachol. The EPP shown on the left was recorded after 10 min of toxin exposure, as soon as muscle contractions had stopped. The middle trace, recorded after 30 min of toxin exposure, shows almost complete block of the EPP, consistent with previous demonstrations that 1–5 μM ω-conotoxin GVIA blocks transmitter release (as well as Ca^{2+}-dependent potentials) originating from lizard motor nerve terminals (Angaut-Petit *et al.* 1989; Lindgren & Moore, 1989, 1991; Morita & Barrett, 1989). Toxin inhibition of the $\Delta F/F$ transient and the EPP was slowly reversible (over a period of hours; see Barhanin, Schmid & Lazdunski, 1988; Yoshikami, Bagabaldo & Olivera, 1989).

The right trace in Fig. 5*C* shows that addition of 3,4-DAP markedly increased the EPP recorded in conotoxin; in fact, the muscle contracted shortly after this record was obtained. This latter result suggests that the toxin-resistant component of the $\Delta F/F$ transient shown in Fig. 5*B* was capable of supporting substantial phasic evoked release.

Simultaneous measurement of fluorescence transients and EPPs

Figure 6*A* and *B* shows for a fluo-3-filled terminal that in the absence of K^+ channel blocking agents the amplitude of the EPP and $\Delta F/F$ transient remained roughly equal for each of four stimuli in a 50 Hz train. Figure 6*C* and *D* shows that in another terminal filled with Oregon Green BAPTA-5N and bathed in 3,4-DAP, the EPPs evoked by later stimuli in the train were greatly depressed, but the $\Delta F/F$ transient associated with each stimulus remained roughly constant. This result suggests that EPP depression is not caused by decreased Ca^{2+} entry. A similar conclusion was reached in studies of Ca^{2+} currents at the squid giant synapse (Charlton, Smith & Zucker, 1982) and perineurial recordings at the frog neuromuscular junction (Redman & Silinsky, 1994). Depression may have been due in part to depletion of readily releasable vesicles, since aminopyridines greatly increase transmitter release from motor terminals (e.g. Heuser, Reese, Dennis, Jan, Jan & Evans, 1979). Transmitter release declined more rapidly than the fluorescence transient, as also noted at other phasically releasing synapses (see Introduction).

Figure 7 shows EPPs and the early time course of $\Delta F/F$ transients recorded in boutons filled with fluo-3 in normal saline (*A*) or with Oregon Green BAPTA-5N in the presence of 3,4-DAP (*B*). In both cases the $\Delta F/F$ transients led the EPP, as would be expected if Ca^{2+} entry precedes the onset of transmitter release. The $\Delta F/F$ transient recorded with fluo-3 reached its peak considerably later than that recorded with Oregon Green BAPTA-5N. This difference is due at least in part to the differing Ca^{2+} binding kinetics of these dyes (see Regehr & Atluri, 1995). The fraction of the higher affinity indicator (fluo-3) binding Ca^{2+} would be expected to continue to increase for some time after Ca^{2+} entry stops, whereas the fraction of the lower affinity indicator (Oregon Green BAPTA-5N) binding Ca^{2+} would be expected to stop increasing shortly after Ca^{2+} entry ends.

Measured $\Delta F/F$ transients are expected to have a slower time course than the underlying $[Ca^{2+}]_i$ transients, due in part to the kinetics of dye–Ca^{2+} binding. To estimate how dye kinetics might affect $[Ca^{2+}]_i$ values calculated from measured $\Delta F/F$ transients, we applied eqn (2) to the data of Fig. 7 (see Methods). For the fluo-3 data of Fig. 7*A*, eqn (2) yielded a $[Ca^{2+}]_i$ transient that peaked at an earlier time than the measured $\Delta F/F$ transient (1·5 instead of ⩾ 9 ms after stimulus onset, not shown), and reached a greater peak magnitude than that calculated without correction for dye kinetics (59 instead of 36 nM). Application of eqn (2) to the Oregon Green BAPTA-5N data of Fig. 7*B* yielded corrections of peak amplitude and time course that were in the same direction, but were quantitatively much smaller (reduction in time of peak from 2·1 to 2·0 ms after stimulus onset, ⩽ 5% increase in peak $\Delta[Ca^{2+}]_i$). Thus the $\Delta F/F$ transient measured with low affinity dyes appears to yield a closer approximation to the magnitude and time course of

the underlying changes in $[Ca^{2+}]_i$ than that measured with high affinity dyes. A corollary of this conclusion is that the higher estimates of peak amplitude obtained with the low affinity dye Oregon Green BAPTA-5N (Table 1) are more accurate than the lower estimates obtained with higher affinity dyes.

DISCUSSION

Localization of action potential-induced $[Ca^{2+}]_i$ increase to boutons

Lizard motor boutons showed prominent $\Delta F/F$ transients in response to nerve stimulation, and these transients were similar for boutons within a given motor terminal (Fig. 1*C*). This uniformity suggests that $\Delta F/F$ transients measured from line scans through single boutons are representative of transients occurring in all boutons of that terminal. The finding that much of the $\Delta F/F$ transient was blocked by ω-conotoxin GVIA, which blocks high-voltage-activated Ca^{2+} channels, suggests that nerve stimulation normally produces large depolarizations in terminal boutons.

Stimulation-evoked $\Delta F/F$ transients were much larger in boutons than in the preterminal motor axon (compare red and green traces in Fig. 1*C*). Borst *et al.* (1995) also reported a severalfold larger $\Delta F/F$ transient in Calcium Green-5N-filled calyciform terminals of the rat medial nucleus of the trapezoid body than in the preterminal axon. They saw rapidly rising $\Delta F/F$ transients in the preterminal axon in response to single stimuli (their Fig. 9), suggesting the presence of some Ca^{2+} channels in the preterminal membrane. In contrast, we never detected a fluorescence increase in preterminal motor axons in response to single stimuli, even with higher affinity dyes in the presence of 3,4-DAP, and the $\Delta F/F$ transients measured in preterminal axons after multiple stimuli at 50 Hz rose much more slowly than those in the terminal boutons. These results suggest that in motor axons the main source of the stimulation-induced increase in preterminal $[Ca^{2+}]_i$ was diffusion of Ca^{2+} from sites of entry in the boutons, rather than entry via Ca^{2+} channels on the preterminal axolemma.

Lizard motor boutons, connected to each other and to the preterminal axon by thin processes, may form compartments in which changes in $[Ca^{2+}]_i$ can occur relatively independently of those in neighbouring boutons. In fact, when a peripherally located dye-loaded bouton was subjected to excessive focal irradiation, leading to elevation of $[Ca^{2+}]_i$ in that bouton and eventual bouton disintegration, the $[Ca^{2+}]_i$ in the remaining boutons of that terminal remained near normal (not shown). This ability of motor boutons to form relatively isolated compartments is reminiscent of the ability of dendritic spines to form a compartment isolated from the main dendritic shaft (Petrozzino, Pozzo Miller & Connor, 1995; Segal, 1995; Svoboda, Tank & Denk, 1996).

Nature of depolarization-activated Ca^{2+} channels in lizard motor nerve terminals

ω-Conotoxin GVIA, a toxin selective for N-type Ca^{2+} channels, blocked almost completely the EPP recorded in physiological saline (Fig. 5*C*) as well as the majority of the stimulation-induced $\Delta F/F$ transient recorded in 3,4-DAP (Fig. 5*B*). Thus the Ca^{2+} channels most closely associated with transmitter release from lizard motor terminals exhibit N-type pharmacology. N-type Ca^{2+} channels have been linked to exocytotic release in a variety of synaptic preparations (reviewed by Dunlap, Luebke & Turner, 1995).

Even after prolonged exposure to high toxin concentrations (5–10 μM), terminals bathed in 3,4-DAP exhibited substantial EPPs as well as substantial $\Delta F/F$ transients measured with high affinity dye. At least part of this conotoxin resistance is probably due to non-competitive inhibition of toxin binding by bath cations, especially Ca^{2+} (Abe, Koyano, Saisu, Nishiuchi & Sakakibara, 1986; Barhanin *et al.* 1988; Wagner, Snowman, Biswas, Olivera & Snyder, 1988; Witcher, De Waard & Campbell, 1993). It is also possible that lizard motor terminal membranes contain more than one type of depolarization-activated Ca^{2+} channel. The somatic membranes of vertebrate motoneurones contain multiple types of high-voltage-activated Ca^{2+} channels (e.g. rat hypoglossal motoneurones; Umemiya & Berger, 1995).

Estimates of stimulation-induced $\Delta[Ca^{2+}]_i$ and spatial $[Ca^{2+}]_i$ gradients

Calculations based on measured $\Delta F/F$ transients suggest that following a single action potential the spatially averaged $[Ca^{2+}]_i$ increased by up to 150 nM in normal (carbachol-containing) saline, and by up to 940 nM in the presence of 3,4-DAP (Table 1). The value in normal saline is within the 5–400 nM range calculated from measurements in other small presynaptic terminals filled with indicator dyes (reviewed in Regehr & Atluri, 1995; also Feller, Delaney & Tank, 1996; Helmchen, Borst & Sakmann, 1997). These values are insufficient to account for the difference between the rates of spontaneous and phasic evoked release: assuming a resting $[Ca^{2+}]_i$ no less than 50 nM, an average $\Delta[Ca^{2+}]_i$ of $\leqslant 150$ nM would at most quadruple $[Ca^{2+}]_i$, predicting a 256-fold increase in release rate assuming a fourth power relationship between $[Ca^{2+}]_i$ and transmitter release (Dodge & Rahamimoff, 1967). The actual increase in release rate of about 10^5-fold at neuromuscular junctions (from $\sim 1\ s^{-1}$ for spontaneous release to 100 quanta released in 1 ms during peak evoked release) would predict at least an 18-fold increase ($= (10^5)^{1/4}$) in $[Ca^{2+}]_i$ near release sites. These and other considerations have led to the hypothesis that activation of phasic evoked release requires $[Ca^{2+}]_i$ of at least 10–300 μM (Simon & Llinás, 1985; Smith & Augustine, 1988 (review); Adler, Augustine, Duffy & Charlton, 1991; Yamada & Zucker, 1992; Landó & Zucker,

1994), and $[Ca^{2+}]_i$ in this range has been measured in retinal bipolar cell terminals (Heidelberger, Heinemann, Neher & Matthews, 1994) and in localized regions within stimulated squid giant presynaptic terminals (Llinás *et al.* 1992).

A major reason why the $\Delta F/F$ measurements presented here underestimate the peak stimulation-induced $\Delta[Ca^{2+}]_i$ near release sites is the spatial gradients of $[Ca^{2+}]_i$ within the bouton at early poststimulation times. Using an equation for characteristic diffusion time (τ_{ch}) from Atluri & Regehr (1996):

$$\tau_{ch} = r^2/6D,$$

where r is bouton radius and D is the effective diffusion coefficient for Ca^{2+} in cytoplasm (1×10^{-7} cm^2 s^{-1}), the predicted equilibration time for lizard motor boutons 2–5 μm in diameter is 17–100 ms. Figure 4 shows an experimental demonstration of this predicted spatial $[Ca^{2+}]_i$ gradient, manifested as a $\Delta F/F$ gradient between the edge and centre of a 4 μm diameter bouton. The duration of this poststimulation $\Delta F/F$ gradient ($\geqslant$ 15 ms) is close to that predicted by the above equation. To our knowledge this is the smallest structure in which a transient poststimulation spatial $[Ca^{2+}]_i$ gradient has been demonstrated.

This illustrated gradient underestimates the true spatial gradient, for several reasons. First, peak $\Delta F/F$ values averaged over the outer third of the bouton must underestimate peak values near the inner mouth of an open Ca^{2+} channel. Our spatial gradient measurement could not differentiate between uniform Ca^{2+} influx throughout the presynaptic membrane and more localized domains of Ca^{2+} entry. However, freeze fracture replicas of motor terminals on lizard twitch muscles showing exocytotic release sites situated between two parallel paired rows of large membrane particles (some of which may be Ca^{2+} channels) arranged in ~80 nm × 80 nm clusters on the presynaptic membrane (Walrond & Reese, 1985) favour the domain hypothesis. Rapidly collapsing local domains of elevated $[Ca^{2+}]_i$ around release sites might also help explain the fact that measured $\Delta F/F$ transients decay much more slowly than the EPP (Fig. 7).

The presence of the dye as a diffusible Ca^{2+} buffer will also cause the measured spatial $\Delta F/F$ gradient to underestimate the spatial $[Ca^{2+}]_i$ gradient at early times, to the extent that the calcium–dye complex diffuses in cytoplasm faster than free Ca^{2+} (Sala & Hernández-Cruz, 1990). This error is expected to be more prominent with higher affinity dyes (slower dissociation constants), because the calcium–dye complex that diffuses from sub-membrane regions to the centre of the bouton will take longer to equilibrate with the lower $[Ca^{2+}]_i$ in the centre. Consistent with this prediction, we were unable to detect a spatial $\Delta F/F$ gradient at early times in boutons filled with high affinity dyes, but were able to detect such a gradient in boutons filled with a low affinity dye.

Abe, T., Koyano, K., Saisu, H., Nichiuchi, Y. & Sakakibara, S. (1986). Binding of ω-conotoxin to receptor sites associated with the voltage-sensitive calcium channel. *Neuroscience Letters* **71**, 203–208.

Adler, E. M., Augustine, G. J., Duffy, S. N. & Charlton, M. P. (1991). Alien intracellular calcium chelators attenuate neurotransmitter release at the squid giant synapse. *Journal of Neuroscience* **11**, 1496–1507.

Angaut-Petit, D., Benoit, E. & Mallart, A. (1989). Membrane currents in lizard motor nerve terminals and nodes of Ranvier. *Pflügers Archiv* **415**, 81–87.

Atluri, P. P. & Regehr, W. G. (1996). Determinants of the time course of facilitation at the granule cell to Purkinje cell synapse. *Journal of Neuroscience* **16**, 5661–5671.

Augustine, G. J., Charlton, M. P. & Smith, S. J. (1987). Calcium action in synaptic transmitter release. *Annual Review of Neuroscience* **10**, 633–693.

Barhanin, J., Schmid, A. & Lazdunski, M. (1988). Properties of structure and interaction of the receptor for ω-conotoxin, a polypeptide active on Ca^{2+} channels. *Biochemical and Biophysical Research Communications* **150**, 1051–1062.

Borst, J. G. G., Helmchen, F. & Sakmann, B. (1995). Pre- and postsynaptic whole-cell recordings in the medial nucleus of the trapezoid body of the rat. *Journal of Physiology* **489**, 825–840.

Brain, K. L. & Bennett, M. R. (1995). Calcium in the nerve terminals of chick ciliary ganglia during facilitation, augmentation and potentiation. *Journal of Physiology* **489**, 637–648.

Brigant, J. L. & Mallart, A. (1982). Presynaptic currents in mouse motor endings. *Journal of Physiology* **333**, 619–636.

Charlton, M. P., Smith, S. J. & Zucker, R. S. (1982). Role of presynaptic calcium ions and channels in synaptic facilitation and depression at the squid giant synapse. *Journal of Physiology* **323**, 173–193.

Cheng, H., Lederer, W. J. & Cannell, M. B. (1993). Calcium sparks: elementary events underlying excitation-contraction coupling in heart muscle. *Science* **262**, 740–744.

David, G., Barrett, J. N. & Barrett, E. F. (1996). Fluorescence imaging of stimulation-induced $[Ca^{2+}]$ changes in lizard motor nerve terminals. *Society for Neuroscience Abstracts* **22**, 775.

David, G., Barrett, J. N. & Barrett, E. F. (1997). Spatiotemporal gradients of intra-axonal $[Na^+]$ after transection and resealing in lizard peripheral myelinated axons. *Journal of Physiology* **498**, 295–307.

Delaney, K. R., Zucker, R. S. & Tank, D. W. (1989). Calcium in motor nerve terminals associated with posttetanic potentiation. *Journal of Neuroscience* **9**, 3558–3567.

Dodge, F. A. & Rahamimoff, R. (1967). Co-operative action of calcium ions in transmitter release at the neuromuscular junction. *Journal of Physiology* **193**, 419–432.

Dunlap, K., Luebke, J. I. & Turner, T. J. (1995). Exocytotic Ca^{2+} channels in mammalian central neurons. *Trends in Neurosciences* **18**, 89–98.

Eilers, J., Callewaert, G., Armstrong, C. & Konnerth, A. (1995). Calcium signaling in a narrow somatic submembrane shell during synaptic activity in cerebellar Purkinje neurons. *Proceedings of the National Academy of Sciences of the USA* **92**, 10272–10276.

Feller, M. B., Delaney, K. R. & Tank, D. W. (1996). Presynaptic calcium dynamics at the frog retinotectal synapse. *Journal of Neurophysiology* **76**, 381–400.

Grynkiewicz, G., Poenie, M. & Tsien, R. Y. (1985). A new generation of Ca^{2+} indicators with greatly improved fluorescence properties. *Journal of Biological Chemistry* **260**, 3440–3450.

HEIDELBERGER, R., HEINEMANN, C., NEHER, E. & MATTHEWS, G. (1994). Calcium dependence of the rate of exocytosis in a synaptic terminal. *Nature* **371**, 513–515.

HELMCHEN, F., BORST, J. G. G. & SAKMANN, B. (1997). Calcium dynamics associated with a single action potential in a CNS presynaptic terminal. *Biophysical Journal* **72**, 1458–1471.

HEUSER, J. E., REESE, T. S., DENNIS, M. J., JAN, Y., JAN, L. & EVANS, L. (1979). Synaptic vesicle exocytosis captured by quick freezing and correlated with quantal transmitter release. *Journal of Cell Biology* **81**, 275–300.

KATZ, B. (1969). *The release of neural transmitter substances.* Sherrington Lecture No. 10. Liverpool University Press, Liverpool, UK.

KLINGAUF, J. & NEHER, E. (1997). Modeling buffered Ca^{2+} diffusion near the membrane: implications for secretion in neuroendocrine cells. *Biophysical Journal* **72**, 674–690.

LANDÓ, L. & ZUCKER, R. S. (1994). Ca^{2+} cooperativity in neurosecretion measured using photolabile Ca^{2+} chelators. *Journal of Neurophysiology* **72**, 825–830.

LATTANZIO, F. A. JR & BARTSCHAT, D. K. (1991). The effect of pH on rate constants, ion selectivity and thermodynamic properties of fluorescent calcium and magnesium indicators. *Biochemical and Biophysical Research Communications* **177**, 184–191.

LINDGREN, C. A. & MOORE, J. W. (1989). Identification of ionic currents at presynaptic nerve endings of the lizard. *Journal of Physiology* **414**, 201–222.

LINDGREN, C. A. & MOORE, J. W. (1991). Calcium current in motor nerve endings of the lizard. *Annals of the New York Academy of Sciences* **635**, 58–68.

LLINÁS, R., SUGIMORI, M. & SILVER, R. B. (1992). Microdomains of high calcium concentration in a presynaptic terminal. *Science* **256**, 677–679.

MALLART, A. (1985). A calcium-activated potassium current in motor nerve terminals of the mouse. *Journal of Physiology* **368**, 577–591.

MELAMED, N. & RAHAMIMOFF, R. (1991). Confocal microscopy of the lizard motor nerve terminals. *Journal of Basic and Clinical Physiology and Pharmacology* **2**, 63–85.

MILEDI, R. & PARKER, I. (1981). Calcium transients recorded with arsenazo III in the presynaptic terminal of the squid giant synapse. *Proceedings of the Royal Society* B **212**, 197–211.

MORITA, K. & BARRETT, E. F. (1989). Calcium-dependent depolarizations originating in lizard motor nerve terminals. *Journal of Neuroscience* **9**, 3359–3369.

MORITA, K. & BARRETT, E. F. (1990). Evidence for two calcium-dependent potassium conductances in lizard motor nerve terminals. *Journal of Neuroscience* **10**, 2614–2625.

PARNAS, H. & PARNAS, I. (1994). Neurotransmitter release at fast synapses. *Journal of Membrane Biology* **142**, 267–279.

PETROZZINO, J. J., POZZO-MILLER, L. D. & CONNOR, J. A. (1995). Micromolar Ca^{2+} transients in dendritic spines of hippocampal pyramidal neurons in brain slice. *Neuron* **14**, 1223–1231.

REDMAN, R. S. & SILINSKY, E. M. (1994). ATP released together with acetylcholine as the mediator of neuromuscular depression at frog motor nerve endings. *Journal of Physiology* **477**, 117–127.

REGEHR, W. G. & ATLURI, P. P. (1995). Calcium transients in cerebellar granule cell presynaptic terminals. *Biophysical Journal* **68**, 2156–2170.

SALA, F. & HERNÁNDEZ-CRUZ, A. (1990). Calcium diffusion modeling in a spherical neuron: relevance of buffering properties. *Biophysical Journal* **57**, 313–324.

SEGAL, M. (1995). Imaging of calcium variations in living dendritic spines of cultured rat hippocampal neurons. *Journal of Physiology* **486**, 283–295.

SIMON, S. M. & LLINÁS, R. R. (1985). Compartmentalization of the submembrane calcium activity during calcium influx and its significance in transmitter release. *Biophysical Journal* **48**, 485–498.

SMITH, S. J. & AUGUSTINE, G. J. (1988). Calcium ions, active zones and synaptic transmitter release. *Trends in Neurosciences* **11**, 458–464.

SVOBODA, K., TANK, D. W. & DENK, W. (1996). Direct measurement of coupling between dendritic spines and shafts. *Science* **272**, 716–719.

TUCKER, T. & FETTIPLACE, R. (1995). Confocal imaging of calcium microdomains and calcium extrusion in turtle hair cells. *Neuron* **15**, 1323–1336.

TUCKER, T. R. & FETTIPLACE, R. (1996). Monitoring calcium in turtle hair cells with a calcium-activated potassium channel. *Journal of Physiology* **494**, 613–626.

UKHANOV, K. Y., FLORES, T. M., HSIAO, H.-S., MOHAPATRA, P., PITTS, C. H. & PAYNE, R. (1995). Measurement of cytosolic Ca^{2+} concentration in Limulus ventral photoreceptors using fluorescent dyes. *Journal of General Physiology* **105**, 95–116.

UMEMIYA, M. & BERGER, A. J. (1995). Single-channel properties of four calcium channel types in rat motoneurons. *Journal of Neuroscience* **15**, 2218–2224.

WAGNER, J. A., SNOWMAN, A. M., BISWAS, A., OLIVERA, B. M. & SNYDER, S. H. (1988). ω-Conotoxin GVIA binding to a high-affinity receptor in brain: characterization, calcium sensitivity, and solubilization. *Journal of Neuroscience* **8**, 3354–3359.

WALROND, J. P. & REESE, T. S. (1985). Structure of axon terminals and active zones at synapses on lizard twitch and tonic muscle fibres. *Journal of Neuroscience* **5**, 1118–1131.

WITCHER, D. R., DE WAARD, M. & CAMPBELL, K. P. (1993). Characterization of the purified N-type Ca^{2+} channel and the cation sensitivity of ω-conotoxin GVIA binding. *Neuropharmacology* **12**, 1127–1139.

YAMADA, W. M. & ZUCKER, R. S. (1992). Time course of transmitter release calculated from simulations of a calcium diffusion model. *Biophysical Journal* **61**, 671–682.

YAWO, H. & CHUHMA, N. (1994). ω-Conotoxin-sensitive and -resistant transmitter release from the chick ciliary presynaptic terminal. *Journal of Physiology* **477**, 437–448.

YOSHIKAMI, D., BAGABALDO, Z. & OLIVERA, B. M. (1989). The inhibitory effects of omega-conotoxins on Ca channels and synapses. *Annals of the New York Academy of Sciences* **560**, 230–248.

Acknowledgements

We thank Dr W. G. L. Kerrick for valuable suggestions, and for measuring the K_d values of fluo-3FF and Oregon Green BAPTA-5N, and Jim Gray and Conrado Freites for help with electronics and microscope modifications. Supported by US Public Health Service grant no. NS12404 and NCRR-BRS Shared Instrumentation Grant 1S10RR08368.

Author's email address

G. David: gdavid@newssun.med.miami.edu

Received 27 January 1997; accepted 9 June 1997.